

Measurements of air/water interfaces in plunging breaking waves

C.E. Blenkinsopp and J.R. Chaplin

School of Civil Engineering and the Environment, University of Southampton, UK

Introduction

Of the energy dissipation that takes place in violent breaking waves, some is accounted for by work done against the buoyancy of bubbles, and some by work done in generating splashes that may rise to elevations far above the crest. In deep water the probability of encountering air in such conditions varies from almost zero at large submergences to almost unity at high elevations. Between these extremes in regular long-crested waves, there is a two-dimensional continuum of time-dependent ensemble-averaged void fractions. A detailed knowledge of this distribution would represent a major contribution to a better understanding of the process of wave breaking, but largely for practical reasons, little of this information exists.

Previous studies of air entrainment beneath breaking waves have made use of a variety of techniques including local conductivity probes (Cox & Shin, 2003; Hoque 2002), global conductivity probes (Lamarre & Melville, 1994), acoustic techniques and laser methods (Hwung & Jih, 1993). Many of these have shortcomings such as large measurement volumes, limited sensitivity at at least one end of the range of void fractions, or probes that are significantly intrusive. This paper describes detailed measurements made with an instrument that detects individual air/water interfaces over extremely small areas at high frequency. The results allowed us to compute time-dependent void fractions, not only in that part predominantly occupied by water, but in the region above, including (probably for the first time) the splash-up created by the plunging jet.

Experimental arrangements

This study makes use of a novel optical fibre phase detection probe that relies on the difference between refractive indices of different fluids (see Cartellier & Achard, 1990). The tip of the 10 μ m fibre (the support for which can be seen in figure 1) has a conical shape that acts as a Descartes prism and reflects different intensities of light depending on the refractive index of the medium in which it is immersed. An optical amplifier with a time-resolution of less than 0.033 μ s detected changes in the intensity of the light returning along the optical fibre and in these experiments its output (registering the presence of air or water) was sampled at a rate of 150kHz. Owing to its small size, the probe tip has a negligible effect on the flow, and depending on their speeds can detect bubbles and drops of sizes down to a few microns.

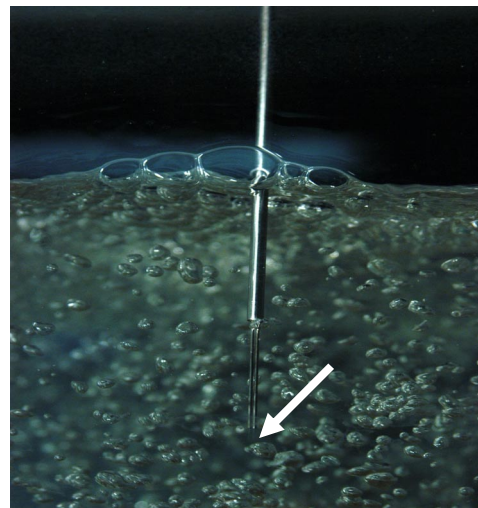


Figure 1. The optical fibre probe. The arrow points to the end of the 10 μ m fibre

The experiments were carried out in a wave flume at the University of Southampton, 17m long, 0.44m wide and filled to a depth of 0.7m. The layout is shown in figure 2. Highly repeatable breaking waves were created over a submerged reef structure with an offshore gradient of 1:10 and a crest height of 0.62m measured from the floor of the tank. The waves broke over the crest of the reef before reforming in the deep water behind it where the measurements were made. The absorbing beach installed in the flume is composed of poly-ether foam, and reduces reflections to around 3%.

The results presented here were obtained using regular waves with a frequency of 0.7Hz and an incident wave height, H_0 of 97.5mm. Measurements were made using two optical fibre probes placed in turn at 560 positions in the vicinity of the breaking wave, in a grid pattern extending horizontally from 80mm ahead of the reef crest to a point 900mm beyond it, and from 220mm below SWL (roughly the greatest depth at which any air bubble was observed) to 100mm above it. The step size in both x (horizontal) and z (vertical) directions was 20mm, and the origin of the grid was at SWL directly above the crest of the reef. For each location, measurements were made through almost 300 waves. Observations over this period showed that the form of the breaking wave varied significantly during the first 6-9 waves but after that became very stable indeed.

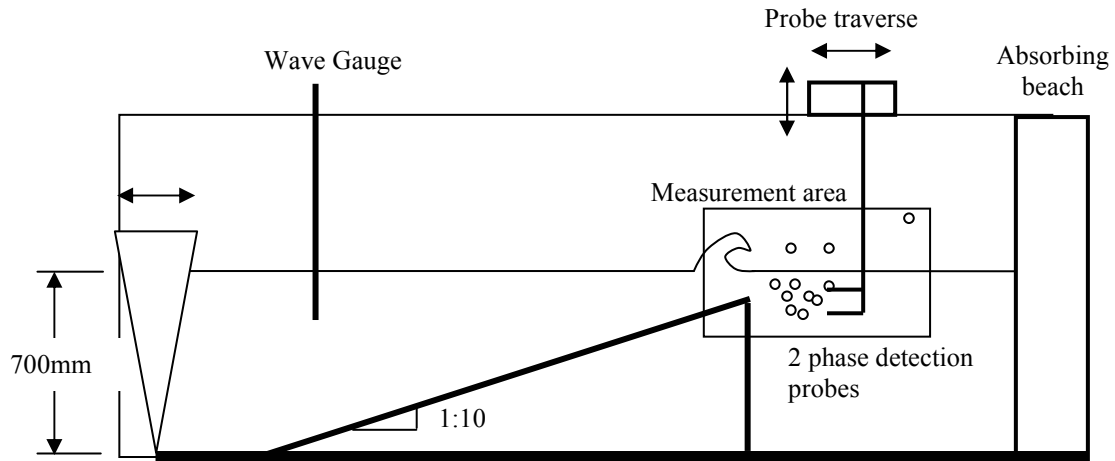


Figure 2. Layout of the experiment

Discussion of results

For present purposes the output of the optic fibre probe can be considered to be $s = 0$ in the presence of water at the tip of the probe and $s = 1$ when it is in air. In each wave period the time series $s(t)$ at each location was divided into 20 equal time bins and the mean value of s in each bin, averaged over all waves, defined a local void fraction $C(x, z, t)$. Contour plots of C at eight times are shown in figure 3 alongside simultaneous images of the breaking wave. The plots show a high degree of compatibility with the images, and reveal quantitatively the evolution of the air below, and the water above, a surface which is identified by the 50% contour. In most cases this marks a steep gradient between regions predominantly of water and air.

Some integral properties of the volume of water above the 50% contour, and the volume of air below it, are shown in figure 4. It can be seen that the total volumes of air and water displaced across this surface are almost equal (though this is not inevitable), but that there is a small time shift between them. The peak volumes are approximately twice that enclosed by the jet of the breaking wave as it first makes contact with the water surface ahead. In figure 4(b) the total potential energies per unit width are shown, and the peak energies associated with elevated water and depressed air are both about 1.25J/m. The combination represents at least 10% of the total energy that is dissipated in each breaking wave. The only previous results with which any of these observations can be compared seem to be those of Lamarre & Melville (1994), who measured only the air entrained at some distance beneath the water surface. In the data of Lamarre & Melville, the total volume of air was comparable to that beneath the initial jet, but the potential energy associated with buoyancy was between 30% and 50% of that of the incoming waves.

The horizontal positions of the centroids of water above and air below the 50% contour are plotted in figure 4(c). Over the early part of the motion, the velocity of advance in both cases is comparable to that of the wave crest.

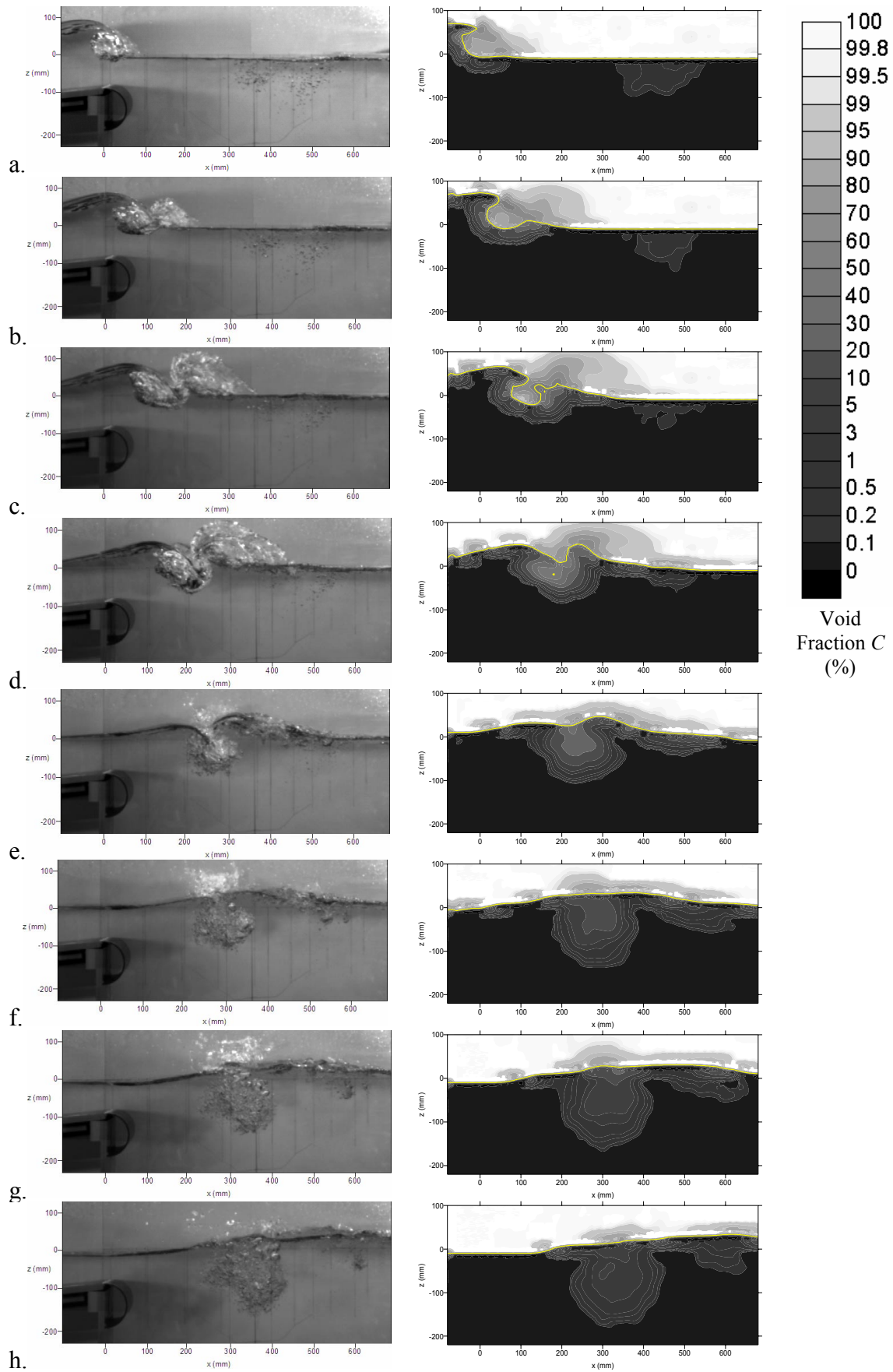


Figure 3. Images (on the left) and simultaneous contour plots of void fractions at 8 phases of the breaking wave. The time at (a) is $t = 0.284$ s. The interval between subsequent frames is 0.071 s.

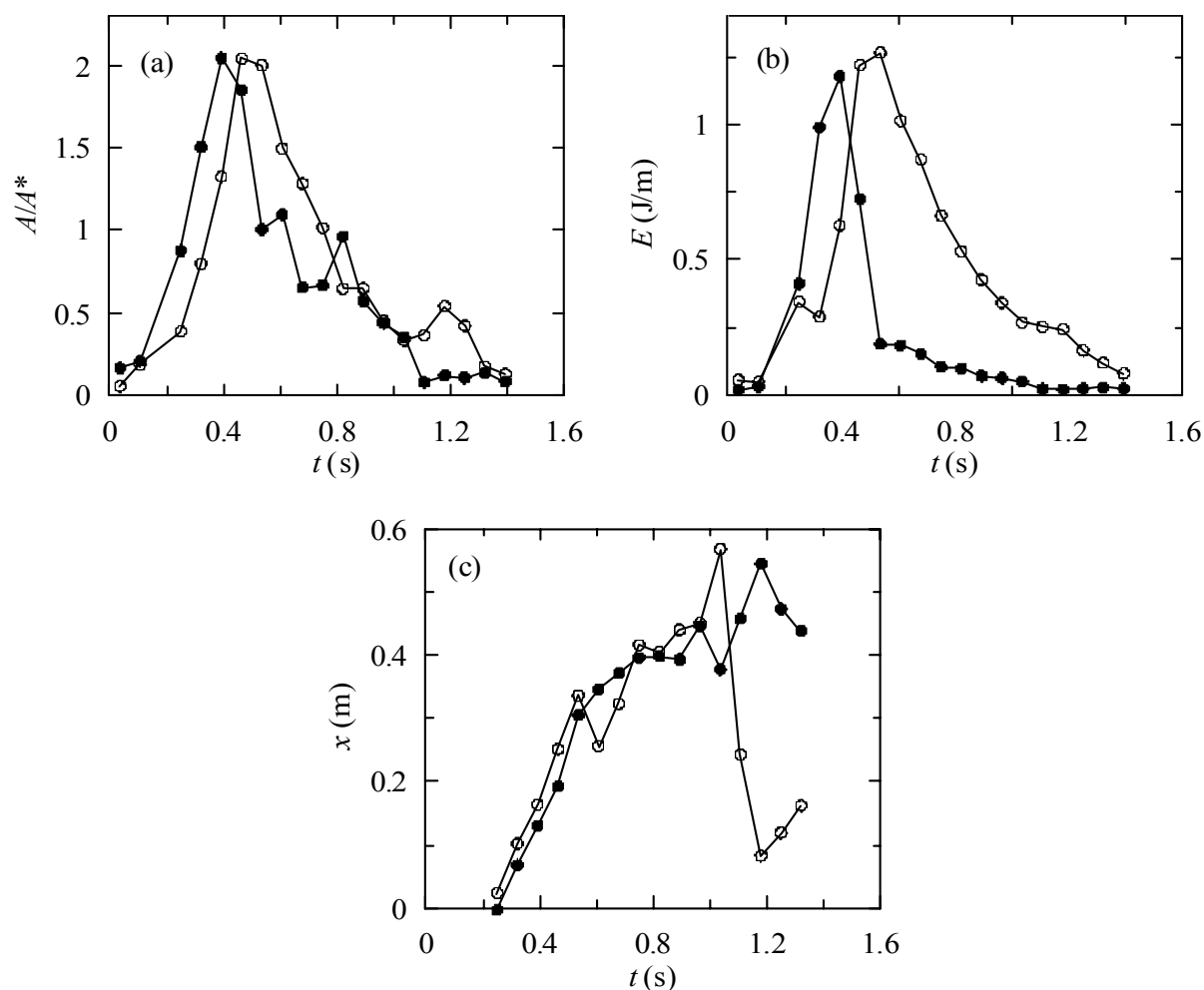


Figure 4. Integral properties of the water above the 50% contour line (shown with solid symbols) and the air below it (shown with empty symbols): (a) the total area (or volume per unit tank width) normalised with respect to A^* , the area enclosed by the jet as it strikes the water surface ahead of the breaking wave; (b) the total potential energy per unit width of water above, and air below, the local elevation of the 50% contour; (c) the position along the x -axis of the centroid of the volumes of water and air, all plotted as functions of time.

References

- Cartellier, A., Achard, J.L., 1990. Local phase detection probes in fluid/fluid two-phase flows. *Review of Scientific Instruments*, 62, 279-303.
- Cox, D. T. and S. Shin, 2003. Laboratory Measurements of Void Fraction and Turbulence in the Bore Region of Surf Zone Waves. *Journal of Engineering Mechanics*, 1197-1205.
- Hoque, A, 2002. Air Bubble Entrainment by Breaking Waves and Associated Energy Dissipation. PhD Thesis, Tokohashi University of Technology.
- Hwung, H. H. and M. C. Jih, 1993. Energy Dissipation and Air Bubbles Mixing Inside Surf Zone. Proceedings of the 23rd International Conference on Coastal Engineering, Vol. 1, 308-321.
- Lamarre, E. and W. K. Melville 1994. Void-fraction Measurements and Sound-Speed Fields in Bubble Plumes Generated by Breaking Waves. *J. Acoust. Soc. Am*, 95(3), 1317-1328.